ADVANCED ENERGY MATERIALS
www.advenergymat.de

Reduction of Graphene Oxide by Hydrogen Sulfide: A Promising Strategy for Pollutant Control and as an Electrode for Li-S Batteries

*Chen Zhang, Wei Lv, Weiguo Zhang, Xiaoyu Zheng, Ming-Bo Wu, Wei Wei, Ying Tao, Zhengjie Li, and Quan-Hong Yang**

The increasing demand for environmentally friendly industries and effective pollution control has attracted great attention from both academic and industrial organizations for the development of new processes and novel materials. As a major air pollutant, hydrogen sulfide (H_2S), originating from various sources (natural gas processing, the refining and consumption of fossil fuel, etc.) must urgently be removed and reused due to its high toxicity towards the environment (acid rain) and living organisms.[1] Great efforts have been made to explore the effective removal of H_2S and in most cases transition-metal oxides and mixed oxides are used as adsorbents and/or catalysts for the oxidation of H_2S, whereas others use zeolite, activated carbon (AC), and carbon nanotubes (CNTs) as adsorbents.[2,3] Carbon materials have appealing properties as adsorbents or catalyst supports for the removal of H_2S. For instance, AC or CNTs have been widely used as supports of catalysts (ZnO, NiS_2, etc.) for the catalytic oxidation of H_2S.[3] Nevertheless, the regeneration and full utilization of the H_2S and the development of high-performance adsorbents are still hard to realize. Thus, it is necessary to develop an appropriate approach to eliminate and recycle H_2S to realize its regeneration and environmental protection.

As a fascinating carbon material, graphene possesses excellent electrical, thermal, and mechanical properties due to its unique 2D structure, making it versatile in fundamental science and various applications, such as energy storage, sensors, adsorption, etc.[4] Due to its large and fully accessible surface and excellent conductivity, the use of graphene in the removal of H_2S has been examined both experimentally and theoretically.[1a,2,5] Density functional theory (DFT) studies show that H_2S molecules are physisorbed only on the surface of graphene, thus, in most cases, graphene has a low catalytic activity for H_2S oxidation and also a low adsorption capacity. Graphene oxide (GO), the most important derivative of graphene, is decorated by abundant oxygen-containing groups on the graphene layer, and these help improve the reactivity and processability due to their hydrophilic nature. Although GO suffers from poor conductivity due to the destruction of the continuous sp^2 hybridized network, it is the most frequently used precursor for the preparation of graphene and graphene-based materials.[6] Some groups have prepared reduced graphene oxide (RGO)/metal oxide composites as adsorbents for H_2S; the oxygen-containing groups of GO help the homogeneous distribution of the metal oxide nanoparticles and the residual oxygen after the reduction of GO can accelerate the catalytic oxidation of H_2S. However, the metal oxide still plays a dominant role in the oxidation of H_2S and the effect of the oxygen in GO is always neglected.[1a,5a,7]

As the main element in H_2S, sulfur attracts much attention nowadays due to its potential for use in high energy density batteries. There is increasing demand for high-performance energy storage devices and the lithium ion battery is constrained by its relatively low energy density. The lithium-sulfur (Li-S) battery, which uses sulfur as the cathode material, has attracted attention for use in electric vehicles and portable devices because of its high energy density and ability to operate for long times.[8] Unfortunately, the poor electric conductivity of sulfur and the dissolution of the polysulfide cause low efficiency and fast capacity fade of the battery. To solve these problems and make the battery usable, S is always combined with a conductive polymer such as polypyrrole (PPy) or a carbon matrix of mesoporous carbon, CNTs or graphene.[9] However, in most cases the uniform distribution of sulfur is hard to realize for high-performance electrode materials.

Here, GO is reduced by H_2S and the concentrated H_2S can be effectively removed by such a reduction process. As a result, a graphene/S hybrid is obtained in which sulfur is uniformly distributed onto graphene layers and graphene layers are interconnected with each other with curly structure. The resultant graphene/S hybrid shows potential for use in a Li-S battery. This strategy realizes a combination of pollutant control and the fabrication of advanced electrode materials for energy storage devices.

C. Zhang, Dr. W. G. Zhang, X. Y. Zheng, W. Wei, Y. Tao
Z. J. Li, Prof. Q.-H. Yang
School of Chemical Engineering and Technology
Tianjin University
Tianjin, 300072, China
E-mail: qhyangcn@tju.edu.cn;
yang.quanhong@mail.sz.tsinghua.edu.cn
C. Zhang, X. Y. Zheng, W. Wei, Y. Tao, Z. J. Li, Prof. Q.-H. Yang
The Synergistic Innovation Center of Chemistry
and Chemical Engineering of Tianjin
Tianjin, 300072, China
Dr. W. Lv, Prof. Q.-H. Yang
Engineering Laboratory for Functionalized Carbon Materials
Graduate School at Shenzhen
Tsinghua University
Shenzhen, 518055, China
Prof. M.-B. Wu
State Key Laboratory of Heavy Oil Processing
China University of Petroleum
Qingdao, 266580, China

DOI: 10.1002/aenm.201301565

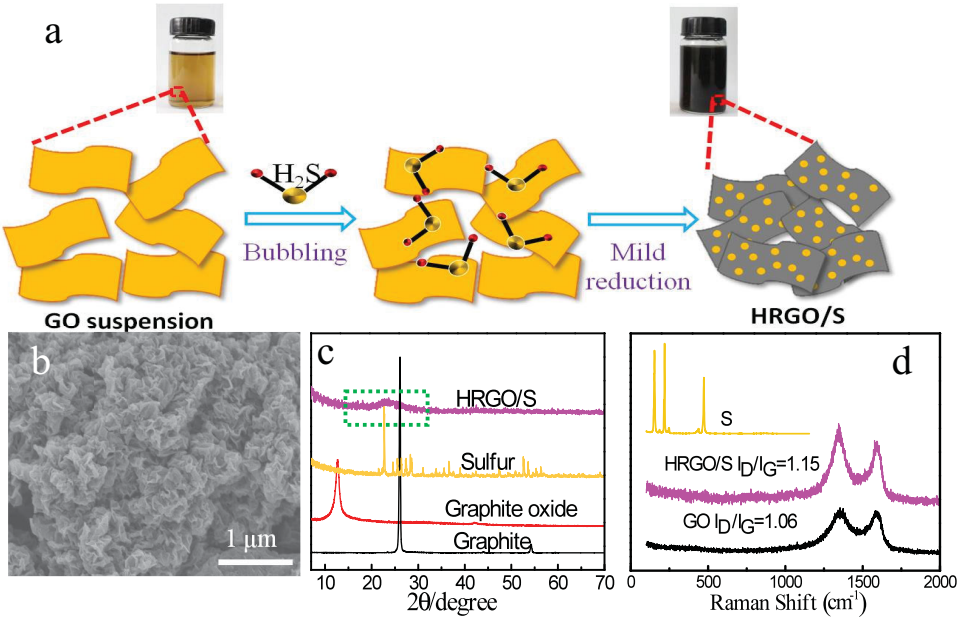

Figure 1. a) Illustration of the formation of HRGO/S hybrid. b) Scanning electron microscopy (SEM) image of HRGO/S. c) XRD patterns of graphite, graphite oxide, sulfur, and HRGO/S. d) Raman spectra of S, HRGO/S, and GO.

The reduction process is illustrated schematically in **Figure 1**a, concentrated H_2S is bubbled continuously into a GO aqueous suspension at 70 °C, and the large number of oxygen-containing groups act as active sites and accelerate the reaction with H_2S. The strategy in this work is highlighted by using H_2S as a reducing agent to realize the reduction of graphene oxide and to obtain a graphene/sulfur hybrid with high sulfur content and a uniform distribution, which is hard to achieve using other methods.[10] Our previous results show that dried GO powder adsorbs very little H_2S due to the insufficient contact and fortunately the GO aqueous suspension helps the monolayer-dispersing of the hydrophilic GO layers ensuring the full contact of H_2S with the surface of GO. After a certain reaction time, GO is deoxygenated to reduced graphene oxide (RGO) and S^{2-} is transformed into elemental S attached to the RGO layers, and the obtained H_2S-reduced graphene oxide/S is denoted HRGO/S. An obvious color change of the GO suspension from bright brown to black is observed after the reaction (top right of Figure 1a), confirming the effective reduction of the GO. A control experiment was conducted without the bubbling of H_2S to verify whether the heating causes the reduction of GO and, as shown in Supporting Information Figure S1, the color does not change after heating under the same conditions but without H_2S bubbling, indicating that no deoxidization occurs and that it is the H_2S that induces the reduction of GO. It is worth noting that the obtained HRGO/S suspension is highly stable and no precipitation occurs after several months. This phenomenon is mainly attributed to the incomplete removal of negatively charged oxygen groups.[6d]

The HRGO/S hybrid is then obtained after drying. Figure 1b clearly shows the curly and interconnected structure of the HRGO/S. The layers are slightly thicker than layers of GO and thermally exfoliated graphene, which results from the effective and homogeneous loading of S on the surface (as shown in the elemental mapping in Supporting Information Figure S2). Such a structure ensures contact between HRGO and S, which facilitates electron transfer when it is used as an electrode material. X-ray diffraction (XRD) results further confirm the effective reduction of GO, which can be identified by the disappearance of the typical diffraction peak of GO located at 12° that is transformed into a broad and weak peak at 26° (the (002) peak of graphite). This is caused by the random and localized stacking of the HRGO, indicating that the loaded S prevents the restacking of graphene layers. In comparison with the XRD pattern of crystalline S, no typical peaks of S in the XRD of HRGO/S can be indexed, indicating that the S exists in a non-crystalline state. No obvious S particles can be observed in the SEM image, also suggesting the non-crystalline state of sulfur. Raman spectra further demonstrate the effective reduction of GO and prove the state of S. As shown in Figure 1d, the intensity ratio of D band and G band (I_D/I_G) of the HRGO/S is higher than that of GO, which is may be due to the increase of the edges during the reduction process, similar to previous reports.[11] It is also interesting that no vibrational mode can be assigned to sulfur in HRGO/S. This is quite distinct from pure S, which has several vibration signals below 500 cm^{-1} (Figure 1d).[9c,12,13] This result agrees well with the XRD analysis, and both reveal the non-crystalline structure of S in the HRGO/S.

To elucidate the chemical composition of HRGO/S and the reduction degree of GO, X-ray photoelectron spectroscopy (XPS) analysis was conducted to obtain precise evidence of the chemical state of each element. An obvious S peak emerges in the full-scan of HRGO/S, and we further fit the C_{1s} peaks to analyze the categories and numbers of functional groups on the HRGO layers. As shown in **Figure 2**a,b, the binding energies of 284.5 and 285.2 eV are attributed to the C=C and C–C bonds, respectively. Moreover, the binding energies of 286.9, 287.5,

Adv. Energy Mater. 2013,
DOI: 10.1002/aenm.201301565

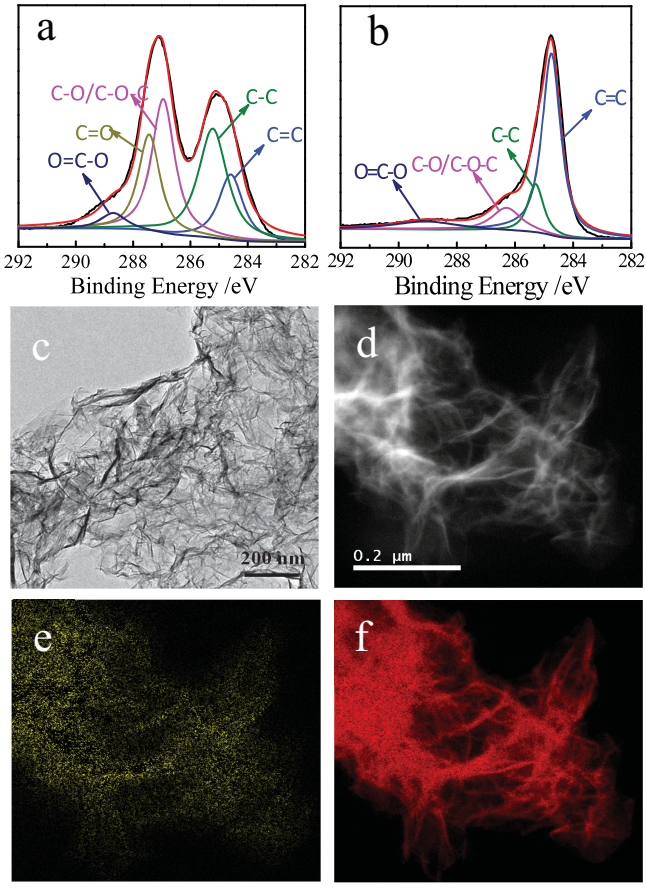

Figure 2. C_{1s} XPS spectra of a) GO and(b) HRGO/S. c) TEM image of HRGO/S. d) Thickness map of HRGO/S by EFTEM. Elemental maps from EFTEM mode of e) element S and f) element C.

and 288.7 eV, respectively, correspond to the C–O, C=O and O=C–O functional groups. Compared with the case of the GO (Figure 2a), the peak intensity of the C=C bond of HRGO/S (located at 284.5 eV) increases significantly accompanied by a dramatic decrease in the intensities of the peaks due to the C–O, C=O and O=C–O bonds, demonstrating the effective restoration of the sp^2 hybridized carbon network.[13] Additionally, the C/O atomic ratio of the GO increased from 1.9 to 9.5 after reduction by H_2S, which is attributed to the reaction between oxygen groups and HS^-.[3a] This result combined with XRD and Raman analyses gives powerful evidence for the effective reduction of the GO by the adsorption of H_2S.

It should be noted that a small number of oxygen-containing groups still exist on the graphene layers, which is a result of the incomplete reduction under mild reduction conditions (<100 °C). In the case of the Li-S battery, these oxygen groups in the HRGO/S should have great help to trap S and limit the dissolution of polysulfide.[13] The above results demonstrated that GO is a promising adsorbent for H_2S and can thus be reduced dramatically to obtain a promising electrode material. Transmission electron microscopy (TEM) analysis gives a more accurate observation for the microstructure of HRGO/S as illustrated in Figure 2c,d. The HRGO/S layers can be identified easily from the TEM images and the relatively low contrast indicates that the HRGO layers are monolayer or few layers (less than four layers, detailed in Supporting Information Figure S3). Numerous dark curves can be observed in Figure 2c, which represent the curly and interconnected structure of the HRGO/S layers. Such a unique structure may be attributed to a slight aggregation of HRGO/S due to its hydrophobic nature after the reduction of GO. The microstructure can be further tuned by the drying process, which is investigated in our ongoing work. Energy-filtered TEM (EFTEM) was used to track the elemental distributions of carbon and sulfur in HRGO/S. The thickness map (Figure 2c) exhibits a more obvious curly and interconnected structure of HRGO/S and the corresponding element maps of C and S (Figure 2e,f) further demonstrate a well-matched spatial distribution. Thus, we believe that S is homogeneously distributed on graphene layers. The S_{2p} XPS spectra further provide detailed information of the chemical state of S in the hybrid. The $S_{2p2/3}$ (163.8 and 165.0 eV) and $S_{2p1/2}$ (164.3 and 165.5 eV) correspond to the S–S bond and S–O bond, respectively, indicating the formation of elemental S. A weak peak located at 168.6 eV can be observed as sulphate species originating from the oxidation of S in air and a trace residue of sulfate.[13] A N_2 adsorption isotherm was also used to analyze the structure and surface area of the HRGO/S. The specific surface area (SSA) of HRGO/S is ≈10 m^2 g^{-1} (Supporting Information Figure S4), which is far lower than exfoliated graphene powder due to the tightly interconnected structure and the loaded S, which cannot contribute to the N_2 adsorption. Although it shows a low SSA, the electrolyte can still fully access the inner surface, which can be proven by the high capacity and power capability resulting from the interconnected structure that provides sufficient ion transportation channels. The sulfur content in this hybrid is estimated of ≈40% (Supporting Information Figure S5), which is the maximum sulfur content even if the the reaction time is prolonged. Differential scanning calorimetry (DSC) measurements (Supporting Information Figure S5) further confirmed the existence of sulfur by the same melting and vaporization temperature (around 290 °C) with pure S, which is in consistence with thermogravimetric (TG) analysis results. To increase the sulfur content, the oxidation state of the graphene oxide should be optimized,[10] and related study is ongoing now.

This strategy for the removal of H_2S not only achieves the elimination of H_2S, but also realizes the in situ preparation of the HRGO/S hybrid. As reported previously, carbon/S hybrids are appealing electrode materials for Li-S batteries,[8] and a graphene-based cathode has been demonstrated as a promising candidate for Li-S batteries. Here, we demonstrate the possibility of HRGO/S as the cathode of a Li-S battery. The electrochemical process, which contains the oxidation of sulfur and the reduction of sulfides in HRGO/S, is illustrated in **Figure 3**b. From the cyclic voltammetry (CV) curves, the reduction peaks located at 2.3 and 2.0 V are two typical reduction potentials of S to a soluble polysulfide and further to the insoluble low-order S^{2-}. Two anodic peaks can be observed at 2.4–2.5 V and are assigned to the oxidation of lithium sulfides to polysulfides and further to element S.[13] The CV results provide solid evidence for the existence of sulfur in the HRGO/S hybrid, as discussed previously, because the redox potential is in good agreement with that of S reported elsewhere. The galvanostatic charge/discharge performance of HRGO/S is evaluated at different

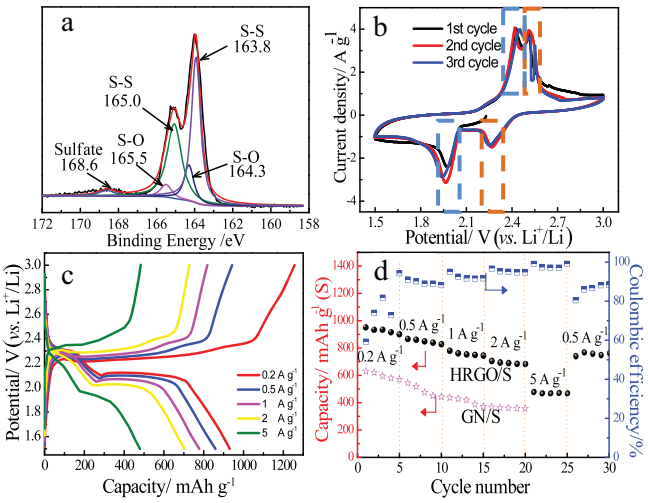

Figure 3. a) S_{2p} XPS spectra of HRGO/S. b) CV curves of HRGO/S at a scan rate of 0.1 mV s^{-1} within a potential range of 1.5–3.0 V. c) Charge–discharge profiles of HRGO/S at different rates. d) Rate performance of HRGO/S and GN/S at different current densities.

current densities (0.2 A g^{-1} to 5 A g^{-1}) within the potential range 1.5–3.0 V. From the charge-discharge profiles at different rates, the voltage plateaus are consistent with the CV curves, indicative of the redox reaction of S. Note that the HRGO/S exhibits good rate performance because the charge/discharge plateaus can be seen clearly even at a high rate (5 A g^{-1}). At a current density of 0.2 A g^{-1}, HRGO/S displays a discharge capacity of 950 mAh g^{-1} (capacity based on the sulfur). With increasing current density, the discharge capacity decreases gradually and a capacity of 683 mAh g^{-1} can be retained at 2.0 A g^{-1}; a capacity of 490 mAh g^{-1} can still be obtained even at 5.0 A g^{-1}. The capacity retention is estimated to be about 72% (2.0 A g^{-1} to 0.2 A g^{-1}), which is far superior to that of a GN/S cathode (melt-diffusion of S with low-temperature thermally exfoliated graphene powder), indicating a better rate performance beyond the traditional GN/S. The homogeneous distribution of S on the tightly curly graphene layers and the presence of oxygen cooperatively are dominantly responsible for the good power performance. When the current density is switched back to 0.5 A g^{-1}, the capacity returns to 761 mAh g^{-1}, which is 92% retention of that of 0.5 A g^{-1} before being subjected to the high rate, indicative of the good stability of the HRGO/S cathode. It also shows relatively stable cyclic ability, and the capacity retention achieves 71% after 100 cycles with a Coulombic efficiency around 94%, which is higher than that of the GN/S (65% retention after 50 cycles and a Coulombic efficiency around 88%; see Supporting Information Figure S6). This may be because of the interaction between the S and the graphene surface derived from chemical reaction process in preparation.

In summary, we have demonstrated the effective reduction of GO and the removal of H_2S can be achieved simultaneously. A homogeneous loading of S on the curly and interconnected graphene layers can be obtained, and the resulting HRGO/S is further highlighted as a possible cathode for Li-S batteries, exhibiting good power performance and stability. It is worth mentioning that this method is a fast and versatile approach for the preparation of a graphene/S hybrid and the structure can be readily controlled. This strategy also hints at an effective adsorption of concentrated H_2S and more detailed work on the adsorption behavior is ongoing. More significantly, this work provides a method for the entirely "green" regeneration of pollutant H_2S gas for use in high-performance Li-S batteries with long life-span and superior power performance.

Supporting Information

Supporting Information is available from the Wiley Online Library or from the author.

Acknowledgements

C.Z. and W.L. contributed equally to this work. The authors appreciate support from National Basic Research Program of China (2014CB932403), National Natural Science Foundation of China (Nos. 513111032 and 51302146); NSF of Tianjin, China (No. 12JCZDJC27400); State Key Laboratory of Heavy Oil Processing, Shenzhen Basic Research Project (No. JC201104210152A) and China Postdoctoral Science Foundation (2013T60111).

Received: October 15, 2013
Revised: November 15, 2013
Published online:

[1] a) H. S. Song, M. G. Park, S. J. Kwon, K. B. Yi, E. Croiset, Z. W. Chen, S. C. Nam, *Appl. Surf. Sci.* **2013**, *276*, 646; b) N. Haimour, R. El-Bishtawi, A. Ail-Wahbi, *Desalination* **2005**, *181*, 145.
[2] J. E. Castellanos Aguila, H. Hernandez Cocoletzi, G. Hernandez Cocoletzi, *AIP Adv.* **2013**, *3*, 032118.
[3] a) M. Seredych, T. J. Bandosz, *Chem. Eng. J.* **2011**, *166*, 1032; b) J. Lin, J. A. May, S. V. Didziulis, E. I. Solomon, *J. Am. Chem. Soc.* **1992**, *114*, 4718; c) C. L. Garcia, J. A. Lercher, *J. Phys. Chem.* **1992**, *96*, 2230; d) J. M. Nhut, P. Nguyen, C. P. Huu, N. Keller, M. J. Ledoux, *Catal. Today* **2004**, *91*, 91; e) R. Yan, D. T. Liang, L. Tsen, J. H. Tay, *Environ. Sci. Technol.* **2002**, *36*, 4460.
[4] a) K. S. Novoselov, A. K. Geim, *Nat. Mater.* **2007**, *6*, 183; b) C. Lee, X. Wei, J. W. Kysar, J. Hone, *Science* **2008**, *321*, 385; c) A. Peigney, C. Laurent, E. Flahaut, R. R. Bacsa, A. Rousset, *Carbon* **2001**, *39*, 507; d) E. J. Yoo, J. Kim, E. Hosono, H. S. Zhou, T. Kudo, I. Honma, *Nano. Lett.* **2008**, *8*, 2277.
[5] a) O. Mabayoje, M. Seredych, T. J. Bandosz, *ACS Appl. Mater. Interfaces* **2012**, *4*, 3316; b) D. Borisova, V. Antonov, A. Proykova, *Int. J. Quantum Chem.* **2013**, *113*, 786; c) H. Huang, P. W. Chen, X. T. Zhang, Y. Lu, W. C. Zhan, *Small* **2013**, *9*, 1397.
[6] a) S. F. Pei, H. M. Cheng, *Carbon* **2012**, *50*, 3210; b) W. Lv, D. M. Tang, Y. B. He, C. H. You, Z. Q. Shi, X. C. Chen, H. M. Cheng, P. X. Hou, C. Liu, Q. H. Yang, *ACS Nano* **2009**, *3*, 3730; c) S. F. Pei, J. P. Zhao, J. H. Du, W. C. Ren, H. M. Cheng, *Carbon* **2010**, *48*, 4464; d) X. B. Fan, W. C. Peng, Y. Li, X. Y. Li, S. L. Wang, G. L. Zhang, F. B. Zhang, *Adv. Mater.* **2008**, *20*, 4490; e) W. Lv, C. H. You, S. D. Wu, B. H. Li, Z. P. Zhu, M. Z. Wang, Q. H. Yang, F. Y. Kang, *Carbon* **2012**, *50*, 3233.
[7] a) H. S. Song, M. G. Park, E. Croiset, Z. W. Chen, S. C. Nam, H. J. Ryu, K. B. Yi, *Appl. Surf. Sci.* **2013**, *280*, 360; b) O. Mabayoje, M. Seredych, T. J. Bandosz, *J. Colloid Interface Sci.* **2012**, *378*, 1.

[8] P. G. Bruce, S. A. Freunberger, L. J. Hardwick, J. M. Tarascon, *Nat. Mater.* **2011**, *11*, 19.
[9] a) X. L. Ji, K. T. Lee, L. F. Nazar, *Nat. Mater.* **2009**, *8*, 500; b) G. C. Li, G. R. Li, S. H. Ye, X. P. Gao, *Adv. Energy. Mater.* **2012**, *2*, 1238; c) G. M. Zhou, D. W. Wang, F. Li, P. X. Hou, L. C. Yin, C. Liu, G. Q. Lu, I. R. Gentle, H. M. Cheng, *Energy. Environ. Sci.* **2012**, *5*, 8901; d) H. L. Wang, Y. Yang, Y. Y. Liang, J. T. Robinson, Y. G. Li, A. Jackson, Y. Cui, H. J. Dai, *Nano. Lett.* **2011**, *11*, 2644.
[10] H. L. Poh, P. Šimek, Z. Sofer, M. Pumera, *ACS Nano* **2013**, *7*, 5262.
[11] S. Stankovich, D. A. Dikin, R. D. Piner, K. A. Kohlhaas, A. Kleinhammes, Y. Y. Jia, Y. Wu, S. T. Nguyen, R. S. Ruoff, *Carbon* **2007**, *45*, 1558; b) F. Tuinstra, J. L. Koenig, *J. Chem. Phys.* **1970**, *53*, 1126.
[12] J. W. Kim, J. D. Ocon, D. W. Park, J. Y. Lee, *J. Energy. Chem.* **2013**, *22*, 336.
[13] a) O. Akhavan, *Carbon* **2010**, *48*, 509; b) Z. Yang, Z. Yao, G. F. Li, G. Y. Fang, H. G. Nie, Z. Liu, X. M. Zhou, X. A. Chen, S. M. Huang, *ACS Nano* **2012**, *6*, 205; c) G. M. Zhou, L. C. Yin, D. W. Wang, L. Li, S. F. Pei, I. R. Gentle, F. Li, H. M. Cheng, *ACS Nano* **2013**, *7*, 5367; d) L. W. Ji, M. M. Rao, H. M. Zheng, L. Zhang, Y. C. Li, W. H. Duan, J. H. Guo, E. J. Cairns, Y. G. Zhang, *J. Am. Chem. Soc.* **2011**, *133*, 18522.